Catalysis Today 213 (2013) 50–57

Contents lists available at SciVerse ScienceDirect

Catalysis Today

journal homepage: www.elsevier.com/locate/cattod

Glycerol steam reforming over Ni/γ-Al_2O_3 catalysts, modified with Mg(II). Effect of Mg (II) content

M.L. Dieuzeide [a], M. Jobbagy [b], N. Amadeo [a,*]

[a] Laboratorio de Procesos Catalíticos, Departamento de Ing. Química, Facultad de Ingeniería, Universidad de Buenos Aires, Pabellón de Industrias, Ciudad Universitaria, 1428 C.A.B.A., Argentina
[b] INQUIMAE, Facultad de Ciencias Exactas y Naturales, Universidad de Buenos Aires, Pabellón II, Ciudad Universitaria, 1428 C.A.B.A., Argentina

ARTICLE INFO

Article history:
Received 24 November 2012
Received in revised form 3 February 2013
Accepted 11 February 2013
Available online 3 April 2013

Keywords:
Glycerol
Ni/γ-Al_2O_3
Mg(II)
Steam reforming

ABSTRACT

Ni based catalysts supported over γ-Al_2O_3, previously modified with increasing contents of Mg(II), were employed for the steam reforming of glycerol. The aim of the present study is to analyze the effect of the content of Mg(II), as a promoter of Ni/γ-Al_2O_3 catalysts, on the textural and structural characteristics of the solid; as well as on the catalytic activity and selectivity to H_2 in the steam reforming of glycerol.

Fresh samples were characterized by PXRD, BET surface area, H_2 chemisorption, TPR, and CO_2-TPD. Used catalysts were analyzed by TPO, in order to study the effect of Mg(II) on carbon gasification. Both fresh and used samples were examined by SEM.

The content of Mg(II) has both an effect on the catalytic performance and on the structural and textural characteristics of the catalysts. The incorporation of Mg(II) results in the formation of $Mg_{1-x}Al_2O_{4-x}$ spinel phase. The differences in catalytic properties due to the increasing content of Mg(II) have effect simultaneously on the Ni° crystallite size, on the acidic–basic character and on the interactions between NiO and support. For the catalysts promoted with Mg(II), the best activity for the steam reforming of glycerol was achieved with Ni(10)Mg(3)Al catalyst while the Ni(10)Mg(15)Al catalyst formed the lowest amount of carbon during reaction time on stream.

The catalyst prepared without Mg(II) presented good activity results despite the lowest Ni dispersion. This behaviour was assigned to the presence of Ni sites more active for the steam reforming of glycerol than the ones on the catalyst promoted with Mg(II). However, this catalyst had the highest carbon deposition during reaction time on stream.

High contents of Mg(II) inhibited carbon formation, this was evidenced by TPO analyses performed to used samples. Low carbon formation at high Mg(II) could be related to the higher basic character of the support as the content of Mg(II) increases.

1. Introduction

In the last decade, production of bio-fuels, such as biodiesel, has increased as a natural response to the concern caused by both the diminishing of non-renewable resources and the increasing global warming effect. Among the bio-fuels one of the most promoted is biodiesel, whose production has grown sharply in recent years. The main biodiesel production process is the transesterification of fats and vegetable oils; glycerol being the major by-product. Consequently, in this scenario the international price of glycerol has fallen sharply, which has prompted the search for alternatives in order to re-valorise this product. Between these alternatives, the steam reforming of glycerol has been proposed in order to produce green hydrogen; being this an economical and effective process with high yields of this outstanding energetic vector that can be easily employed in the fuel cell technology.

The steam reforming of glycerol (GSR) is an endothermic process that takes place according to the following global reaction:

$$C_3H_8O_3 + 3H_2O \rightarrow 7H_2 + 3CO_2 \quad \Delta H^\circ = -123\,kJ/mol$$

Still, the GSR process involves multiple complex reactions, which leads to several intermediate by-products that strongly affect H_2 selectivity. Another key factor lies in the operative conditions under which the reaction takes place. In this sense, a thermodynamic study carried out in a previous paper [1] concluded that in order to both favour H_2 production and minimize carbon formation, the steam reforming of glycerol should be performed at high temperatures, with high feed ratio water to glycerol and at atmospheric pressure.

* Corresponding author. Tel.: +54 1145763212.
E-mail addresses: norma@di.fcen.uba.ar, normaamadeo@yahoo.com.ar (N. Amadeo).

0920-5861/$ – see front matter © 2013 Elsevier B.V. All rights reserved.
http://dx.doi.org/10.1016/j.cattod.2013.02.015

Noble metal based catalysts are commonly used for the steam reforming reaction of hydrocarbons or alcohols [2–7] since they are highly active while they are less susceptible to develop undesired carbon deposits. On the other hand, catalysts based on non-noble transition metals are far cheaper and present higher availability than the former. Among them, Ni based catalysts in particular are known to be active for the cleavage of C—C, O—H and C—H hydrocarbon bonds while they also catalyze water gas shift reaction to remove CO adsorbed from the metallic surface [8–10]. Regarding the supports for Ni, the most usual are based on alumina, carbon or modified alumina with cerium, lanthanum, magnesium or zirconium [9]. However, it is widely known that under the steam reforming of hydrocarbons or alcohols, Ni/Al_2O_3 catalysts suffer deactivation due to the sintering of metallic phase and/or coke deposition [11–15]. In order to minimize coke deposition, several authors proposed the promotion of Ni catalysts supported over alumina by the addition of either alkaline earth oxides or lanthanide oxides [11–13,15–18]. As it has been reported by Cheng et al. [13], the promotion by oxides of the lanthanide group is related to Ni-lanthanide interaction; while the promotion effect of alkaline earth oxides obeys to the weakening of the Ni-alumina interaction. In this sense, it has been suggested that the addition of Mg(II) to Ni/Al_2O_3 catalyst prevents or minimizes carbon formation since it favours the adsorption of H_2O, O_2, CO_2 or —OH fragments, as well as the spillover of such fragments from the support to the metal particles [11,19,20], facilitating carbon gasification. Furthermore, the use of Mg(II) as a promoter in this catalytic system enhances the stability of Ni against sintering [9].

Previously [21], we have studied the influence of the calcination temperature for both the Mg(II)–Al(III) support and the Ni(II) impregnated catalysts, on the activity and selectivity to hydrogen in the GSR reaction. It was concluded that the best catalytic performance was achieved when the modified support had been calcined at 900 °C and the impregnated catalyst had been subsequently calcined at 500 °C. This behaviour is mainly attributed to the formation of Mg(II)–Al(III) spinel-like oxide phase which favours the dispersion of Ni(II), responsible of the catalytic activity.

The main goal of this work is to analyze the effect of the content of Mg(II) in γ-Al_2O_3 modified support, on the activity and on carbon deposition in the GSR. Additionally, it is expected to identify the role of Mg(II) in catalytic activity and in the reduction of carbon formation in the GSR.

2. Experimental

2.1. Catalysts preparation

The catalysts were prepared by the incipient wetness impregnation method. For this purpose aqueous solution of $Mg(NO_3)_2.6H_2O$ (99% Merck) between 2.80 and 14.02 M and $Ni(NO_3)_2.6H_2O$ (99% Merck) 3.87 M were prepared. First, γ-Al_2O_3 (Rhône Poulenc, 200 m^2/g) bare support was impregnated with increasing contents of Mg(II); the samples were dried in a muffle at 120 °C for 6 h, followed by the calcination at 900 °C for another 6 h, according to previous work [21]. Then, each Mg(II)–Al(III) modified support and γ-Al_2O_3, calcined at 900 °C for 6 h, were impregnated with Ni(II), in order to reach a final loading of Ni of 10 wt%; after impregnation the catalysts were dried also at 120 °C for 6 h and calcined at 500 °C for 6 h. During drying and calcinations periods a temperature ramp of 10 °C/min was employed. The catalysts were identified as Ni(10)Mg(x)Al, being x the nominal content of Mg (wt%) between $x = 0$ and 15%.

Prior to impregnation with Mg(II) or Ni(II), γ-Al_2O_3 was crushed and sieved in order to obtain pellets with diameter between 44 μm < dp < 125 μm.

2.2. Characterization

The catalysts were characterized by N_2 sorptometry (BET), Powder X-ray diffraction (PXRD), temperature programmed reduction (TPR), H_2 chemisorption, and temperature programmed desorption of adsorbed CO_2 (CO_2-TPD). The used catalysts were characterized by temperature programmed oxidation (TPO) in order to determine carbon formation. Both fresh and used samples were examined by scanning electron microscopy (SEM).

The characterization by PXRD was performed in Siemens D 5000 equipment, with Cu Kα radiation. BET surface area was obtained in Micromeritics ASAP 2020 equipment.

Temperature programmed reduction (TPR) of the catalysts were carried out in Micromeritics (Autochem II, 2920) equipment, with a thermic conductivity detector (TCD). The fresh samples (100 mg) were placed in a quartz U-shaped tube reactor. Previously to temperature programmed reduction, samples were pre-treated under a flow of Ar (50 mL/min) at 300 °C for 1 h. TPR was performed from 50 °C to 1000 °C, at a heating rate of 10 °C/min, under a flow of 100 mL/min of a mixture 2% H_2/Ar. Hydrogen consumption was determined by a TCD detector and the amount of hydrogen consumed was estimated by the integration of its profile and applying a calibration for H_2.

Metallic surface area and dispersion were obtained by means of H_2 chemisorption in Micromeritics (AutochemII 2920) equipment. The samples (50 mg), placed in a quartz U-shaped reactor, were reduced at 700 °C for an hour under 100 mL/min of a mixture (50:50) H_2/Ar. The chemisorption was performed at 25 °C (keeping this temperature by a flow of nitrogen, which has been previously cooled in a liquid nitrogen bath) by pulses of a mixture of H_2 (10%)/Ar in a flow of 100 mL/min of Ar. The metallic area of Ni was estimated assuming a $Ni_{surface}/H = 1$ stoichiometry and that an atom of Ni occupies 6.49 $Å^2$.

In order to evaluate the distribution of basic sites, the CO_2-temperature programmed desorption (CO_2-TPD) was performed in Micromeritics (Autochem II 2920) equipment. Catalyst samples (50 mg) placed in a quartz U-shaped reactor, were pretreated in a 50 mL/min flow of Ar at 500 °C for an hour, with a temperature ramp of 10 °C/min and then cooled down. CO_2 was adsorbed at 50 °C for an hour from a flow of 100 mL/min of a mixture CO_2:Ar (50:50) and the weakly adsorbed CO_2 was removed by purging with Ar. The sample was heated from 50 °C to 800 °C at a heating rate of 10 °C/min in Ar flow and the desorbed amount of CO_2 was followed by a quadrupole mass spectrometer (m/v = 44). The desorbed CO_2 amount was estimated by integrating the CO_2 profile and applying a CO_2 calibration.

Carbonaceous deposits formed on the catalysts GSR were determined by temperature programmed oxidation (TPO) in a Micromeritics (Autochem II 2920) equipment. Used catalyst samples (20 mg) placed in quartz U-shaped reactor, were pretreated in 50 mL/min of Ar at 300 °C for 30 min and then cooled down. TPO was performed from 50 °C to 800 °C, under 100 mL/min flow of a mixture Air:Ar (25:75), with a temperature ramp of 10 °C/min. The products were followed by a quadrupole mass spectrometer and the only product detected was CO_2 (m/v = 44), indicating that oxidation reaction was complete. The amount of CO_2 produced was estimated by the integration of its profile and by applying a CO_2 calibration.

The morphology of fresh and used samples was examined by scanning electron microscopy (SEM), using an Inspect Scanning Electron Microscope (FEI) operated at 20 kV. Before analysing them, the samples were submitted to metallization with gold in a Emitech K550X equipment.

2.3. Catalytic tests

The catalytic tests were carried out in a stainless-steel continuous flow fixed bed reactor (ϕ = 12 mm) at atmospheric pressure in an electrical furnace equipped with temperature controllers. The contact time (defined on base of glycerol molar flow) was fixed at 3.09 g_{cat} h/$mol_{glycerol}$, reaction temperature was 600 °C; and water to glycerol molar ratio ($R = n_{H_2O}/n_{C_3H_8O_3}$) was 9:1 with a molar fraction of glycerol in the feed mixture of 2%. For all the catalytic tests, 45.5 mg of catalyst were employed, diluted with an inert material in a ratio 10:1. Catalysts were reduced in situ under a flow of 100 mL/min of pure hydrogen with a heating ramp of 10 °C/min to reach 700 °C, keeping this temperature for one hour.

Liquid mixture of water and glycerol was fed to the reactor by a syringe pump (APEMA PC 11U) and it was vaporized in the first third of the reactor. Regarding the carrier gas (Ar) and the reference gas (N_2) they were both fed to the reactor by mass flow controllers (Aalborg AFC).

Moreover, in order to minimize mass transfer effects and ensure catalytic chemical control, based on preliminary tests, particle size was between 44 μm < dp < 125 μm and total feed flow was higher than 200 mL/min.

The gaseous products were analyzed on-line by TCD and FID detectors, in 7890A GC chromatograph of Agilent Technology. Regarding liquid phase products, the stream was continuously condensed and analyzed after four hours of reaction. A CarboxenTM 1010 Plot (30 m × 0.530 mm) column was employed to determine N_2, H_2, CO, CO_2, CH_4 and C_2H_4; while a CP-PoraBOND Q (10 m × 0.32 mm) column was used to analyze the composition of the liquid mixture feed and of the condensed mixture during the reaction.

In order to analyze the catalytic results, the following parameters were considered:

- Glycerol total conversion: $x_T = \frac{F^E_{gly} - F^S_{gly}}{F^E_{gly}} 100$
- Glycerol conversion to gaseous products: $x_G = \frac{\sum Fc_i}{3F^E_{gly}} 100$

With Fc_i: CO2, CO and CH_4

- Glycerol conversion to liquid products: $x_L = x_T - x_G$
- Yields: $Y_i = \frac{F_i}{F^E_{gly}}$

With F_i: H_2, CO_2, CO and CH_4.

The kinetics results that are reported in this work correspond to steady state condition and the experimental dispersion was estimated in 4%.

3. Results and discussion

PXRD inspection of the Mg(II) modified supports, revealed a continuous shift from the parent γ-Al_2O_3 (PDF-10-0425) structure to the stoichiometrical $MgAl_2O_4$ (PDF-21-1152) (Fig. 1.). Intermediate loadings resulted in the formation of its corresponding spinel-like phase ($Mg_{1-x}Al_2O_{4-x}$) (PDF-45-0528). From the PXRD pattern of the modified support with the highest Mg(II) loading (15 wt.%), it is possible to distinguish reflections associated to MgO (PDF-45-0946); which implies some MgO was segregated at high contents of Mg(II).

The subsequent loading with Ni(II) (Fig. 2) resulted in the segregation of NiO (PDF-65-2901), with no significant changes on the spinel-like phase cell parameters confirming that the low annealing temperature prevented the formation of ternary $Mg_{1-x}Ni_xAl_2O_4$ spinel phases. Furthermore, catalysts with Mg(II) contents varying from 3 wt% to 15 wt% exhibited similar PXRD patterns (Fig. 2).

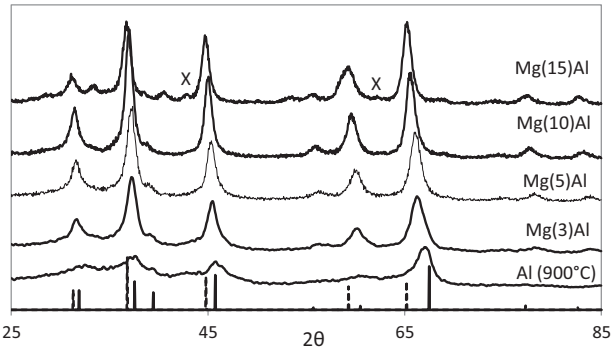

Fig. 1. XRD profiles of Mg/Al_2O_3 modified supports. Mg(*x*)Al, *x* = 0–15 wt.%. Completes line corresponds to γ-Al_2O_3 pattern, dashed line to $MgAl_2O_3$ pattern and (*x*) to MgO.

For Ni(10)Mg(0)Al catalyst (Fig. 2) reflections asoociated with NiO segregation at 2θ = 37.25°, 43.35° and 62.85° (PDF-65-2901) and reflections asociated with Al_2O_3 mainly at 2θ = 67.5° (PDF-10-0425) were observed. Moreover, in Fig. 2 the PXRD pattern of γ-Al_2O_3 calcined at 900 °C has been included, in order to compare it with the PXRD pattern of Ni(10)Mg(0)Al catalyst.

Additionally, Fig. 2 includes a magnification of the region 2θ = 62–70°. It could be observed that both the γ-Al_2O_3 calcined at 900 °C and the catalyst without Mg(II) presented a reflextion at 2θ = 67.5° which is characterictic of γ-Al_2O_3. This result confirms the fact that Ni(II) in this catalyst did not form Ni spinel like phases. For the catalyst promoted with Mg(II) this reflection moved towards lower values of 2θ as Mg(II) content increased, which indicated, as previously mention, the formation of Mg spinel like phases.

Superficial area BET of alumina calcined at 900 °C, of Mg(II) modified supports and of the corresponding Ni(II) catalysts are shown

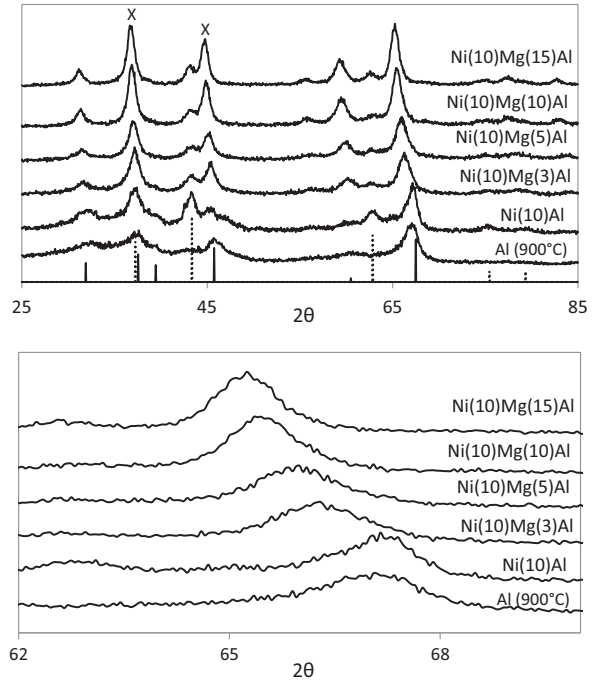

Fig. 2. XRD profiles of the Ni catalysts supported over Mg/Al_2O_3 supports. Ni(10)Mg(*x*)Al, *x* = 0–15% wt, and XRD profile of γ-Al_2O_3 calcined at 900 °C. Completes line corresponds to γ-Al_2O_3 pattern, dashed line to NiO pattern and (*x*) to $NiAl_2O_3$ or $MgAl_2O_3$. A magnification of the region 2θ = 62–70° is included.

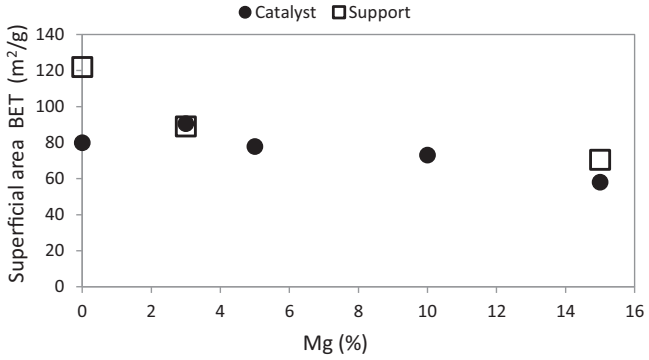

Fig. 3. BET Surface area for both Mg modified support and catalysts, as a function of Mg content.

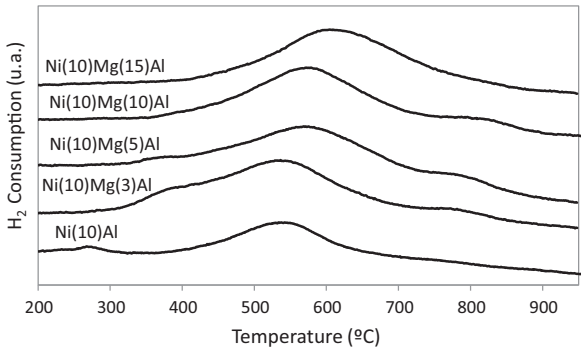

Fig. 4. TPR profiles of the Ni catalyst supported over Mg modified supports. Ni(10)Mg(x)Al, x = 0–15 wt.%.

in (Fig. 3). As the content of Mg(II) increases, the superficial area of the modified supports decreases. This behaviour could be explained by the occlusion of the pores due to $Mg_{1-x}Al_2O_{4-x}$ growth. Also, it can be observed that the surface area of the catalyst with Mg(II) is determined by the surface area of the support modified with the corresponding content of Mg(II). For the Ni(10)Mg(0)Al catalyst a strong decrease in the superficial area is observed, in comparison to the superficial area of alumina calcined at 900 °C, mainly due to the incorporation of Ni(II) into the pores of the alumina.

In Table 1 Ni metallic area, dispersion and particle diameter for all catalysts are presented.

For the catalyst without Mg (II), both Ni metallic area and dispersion were lower and Ni particle diameter higher than the corresponding values obtained for the other catalysts.

The Ni metallic area and dispersion for the catalysts that were modified with Mg(II) (3–15 wt%), were both affected by its content. As Mg(II) loading increased, Ni(II) metallic area and dispersion decreased and consequently the Ni particle diameter increased. It has been previously reported [17] that the promotional effect of Mg(II) addition to alumina support is based on the fact that the precoating of the support (Al_2O_3) with Mg(II) improves metal dispersion as well as stabilizes metal particles against sintering. Furthermore, the formation of Mg(II) spinel phase induces an improvement in the dispersion of metallic Ni. However, from these results it could be seen that both metallic area and dispersion are enhanced at low Mg(II)/Al(III) ratios. Then, the promotional effect of Mg(II) regarding metal area and dispersion is most significant at lower contents of Mg(II). This behaviour agrees with the results presented by Iriondo et al. [11] that at lower loadings of Mg(II), $MgAl_2O_4$ spinel phases are better dispersed, which hinders Ni° particle diffusion and thus promotes higher stability.

In order to determine the reducible species present in each catalyst, TPR tests were conducted between 50 °C and 1000 °C under a flow of H_2 (Fig. 4). The TPR profiles show a broad peak for all catalysts and an additional peak at low temperature for the catalyst without Mg(II). The temperature at the maximum of the broad reduction signal increased (from 535 °C to 610 °C) as the content of Mg(II) increased between 0 wt% and 15 wt%.

Table 1
Results of H_2 chemisorption. Metallic area and dispersion and cristal size of the Ni(10)Mg(x)Al, catalysts, x = 0–15 wt.%.

Catalysts	Metallic dispersion (%)	Metallic area (m^2/g_{sample})	Cubic crystal size (nm)
Ni(10)Al	1.50	0.998	56.29
Ni(10)Mg(3)Al	2.75	1.829	30.71
Ni(10)Mg(5)Al	2.31	1.538	36.54
Ni(10)Mg(10)Al	2.06	1.374	40.88
Ni(10)Mg(15)Al	1.92	1.227	43.99

The reduction profiles could be deconvoluted into four main contributions, which are NiO with weak interaction with the support at a reduction temperature around 370 °C; NiO with moderate interaction with the support, centred on 536 °C; non-stoichiometric $Ni_{1-x}Al_2O_{4-x}$ spinel at 753 °C and stoichiometric Ni spinel at approximately 820 °C [11,12,22]. The predominant phase is, for all catalysts, NiO with moderate interaction with the support, (about 80%).

Particularly, for Ni(10)Mg(0)Al catalyst the signal obtained at 270 °C can be attributed to the reduction of isolated NiO.

It is possible to distinguish that the temperature at the maximum of the reduction peak increased from 535 °C to 610 °C as Mg (II) content increases between 0 wt% and 15 wt%. Similar results have been reported by Iriondo et al. [11]. Since this reduction event is assigned to NiO with moderate interaction with the modified support, it would be possible to attribute the increment in the reduction temperature as Mg (II) content increases to a greater interaction between NiO and MgO. However it is not possible to affirm the formation of a solid solution NiO–MgO due to the low calcination temperature of the catalysts (500 °C) and since it was not possible to distinguish any change in the parameters cell of NiO in PXRD patterns of the catalyst promoted with Mg(II).

The CO_2-TPD profiles for the catalysts Ni(10)Mg(x)Al (x = 0–15 wt%) are shown in Fig. 5. It can be observed that, both the concentration of weak basic sites (occurring at low temperatures) and of strong basic sites (occurring at high temperatures) increase as Mg (II) content increases. In this sense, for the samples without Mg(II) and with 3 wt% of Mg (II), it was only possible to distinguish the presences of weak acid sites in low concentrations. Additionally, it is necessary to remark that for Mg(II) content above 5% the intensity of the CO_2 desorption peaks associated with the presence of weak basic sites is higher than the intensity of the strong ones.

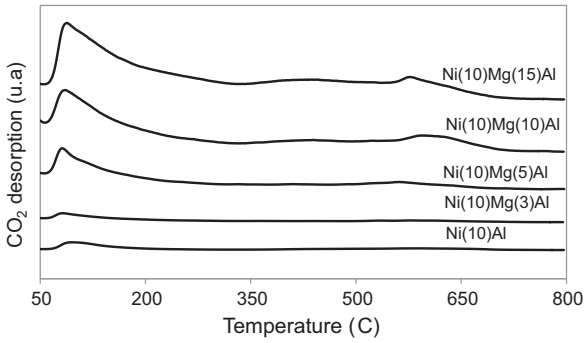

Fig. 5. CO_2-TPD profiles of the Ni catalysts supported over Mg modified supports. Ni(10)Mg(x)Al, x = 0–15 wt.%.

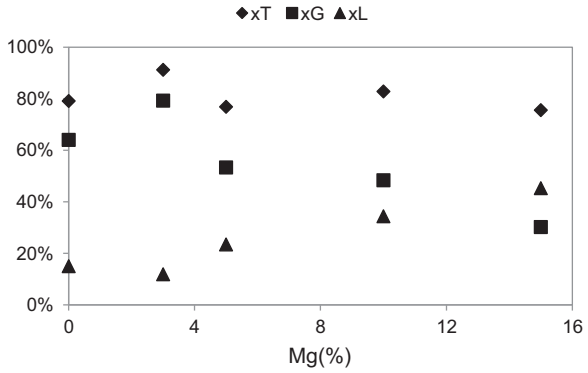

Fig. 6. Glycerol total conversion (x_T), conversion to gaseous products (x_G) and conversion to liquid products (x_L) as a function of Mg content.

GSR activity measurements (Fig. 6) revealed that for the catalysts modified with Mg(II) the glycerol total conversion slightly decreased with the content of Mg(II), while the conversion to gaseous products sharply decreased. With respect to the activity of the catalyst without Mg(II) it can be observed that this was similar to that exhibited by Ni(10)Mg(5)Al catalyst, in spite of its lower Ni dispersion.

The highest conversion to gaseous products (79%) was achieved over Ni(10)Mg(3)Al catalyst and conversion diminished to 30.3%, over Ni(10)Mg(15)Al catalyst. Contrary to what happened with the conversion of glycerol to gaseous products, the glycerol conversion to liquid products ($x_L = x_T - x_G$) increased with Mg(II) loading (Fig. 6).

It is noted that, for the catalysts modified with Mg (II), the conversion of glycerol to gaseous products and the Ni metal dispersion followed the same trend with the content of Mg(II). Thus, the catalyst was more active towards the reforming reactions as Mg(II) content decreased, which would be related to the increase in Ni dispersion.

Instead, the catalytic activity to liquid products was higher as Mg(II) content increased. Similar results were found by Iriondo et al. [11], who correlated the higher content of Mg(II) with lower H_2 yield and with increasing production of liquid oxygenated hydrocarbons. This behaviour deals with the role of intermediate products that liquid oxygenated hydrocarbons [23] present in the steam reforming of glycerol. Therefore, at higher Ni dispersion, there is higher H_2 production and also lower liquid oxygenated hydrocarbon formation; which could be additionally related to the higher activity that Ni has for C—C bond cleavage.

In Fig. 7, the effect of the content of Mg(II) on the distribution of gaseous products is analyzed. The yields to H_2, CO_2 and CO followed the same behaviour as the glycerol conversion to gaseous products. The highest H_2 yield took place with the 3 wt% Mg(II) modified solid

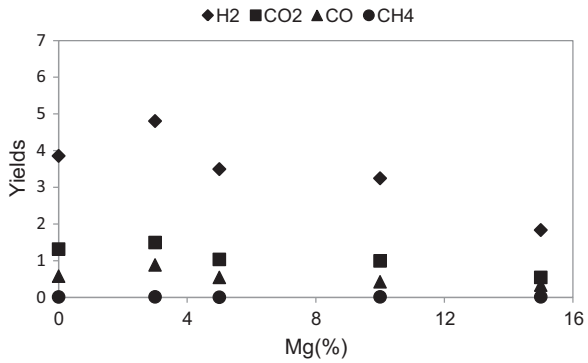

Fig. 7. Gaseous products (H_2, CO_2, CO and CH_4) yields as a function of Mg content.

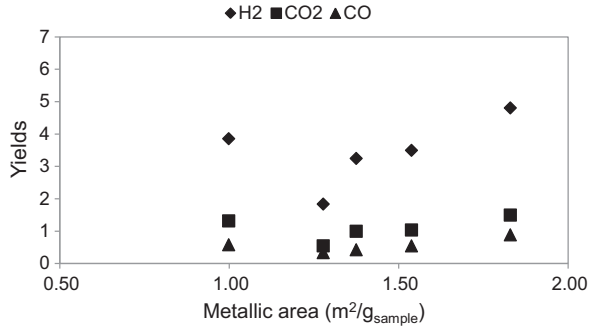

Fig. 8. Gaseous products (H_2, CO_2, CO and CH_4) yields as a function of Ni metallic area.

achieving a yield of 4.8 (76.8% of the thermodynamic yield under these conditions). Beyond this point, H_2 yield decreased with higher Mg(II) contents. With regards to the yields to CH_4 (Fig. 7) and C_2H_4 they were lower than 2%, regardless of the content of Mg(II). The yields to H_2, CO and CO_2 as a function of Ni metallic area are shown in Fig. 8. It is observed that yields to gaseous products increase linearly with Ni metallic area for the catalysts modified with Mg. While a strong deviation from this linear behaviour is detected for the catalyst without Mg (II). The catalyst prepared without Mg(II) has more active Ni sites than the catalyst with Mg(II), which might imply that the presence of $MgAl_2O_4$ modifies the intrinsic activity of Ni°. In this sense, the adverse effect of increasing the amount of Mg(II) added to the alumina, on catalyst activity was reported by Wang et al. [15].

Since the Ni(10)Mg(3)Al catalyst showed the best catalytic performance for the GSR, a stability study for this catalyst was carried out. The reaction conditions were the ones mentioned before; under which the catalyst was stable for a period of 10 h. In Fig. 9 glycerol conversion to gaseous products and H_2 yield values as a function of reaction time are shown.

The effect of Mg(II) content on the formation of carbon was studied by TPO analysis. The samples of catalyst used in the reaction for a period of four hours were analyzed by TPO technique in order to identify and quantify the species of carbon produced.

With regards to the results of TPO for the catalysts with different contents of Mg(II), the TPO profiles for all the catalysts showed the presence of a single species of carbon (Fig. 10). Based on bibliography [24,25], since the formation of CO_2 takes place between 450 °C and 700 °C it was possible to assign this species to filamentous carbon. Additionally, the presence of filamentous carbon is in agreement with the fact that the catalysts did not deactivate under reaction conditions. For the catalysts modified with Mg(II), as the content of Mg(II) increased, a marked decrease in the peak intensity of the CO_2 profile was observed. Besides, it can also be observed a

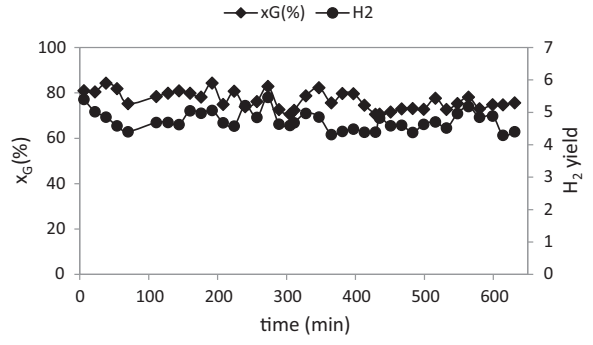

Fig. 9. Stability test. Glycerol conversion to gaseous products (x_G) and hydrogen yield vs. time of reaction.

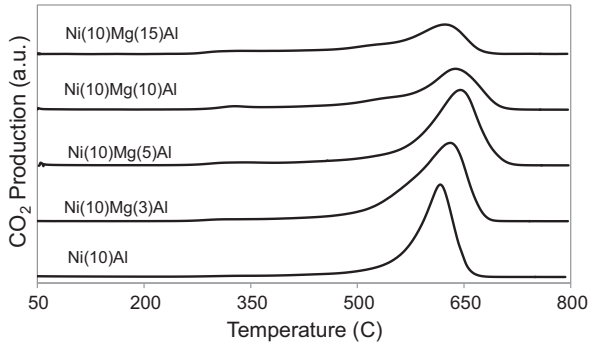

Fig. 10. CO_2-TPO profiles of the Ni catalysts supported over Mg modified supports. Ni(10)Mg(x)Al, x = 0–15 wt.%.

slight decrease in the temperature at which the maximum CO_2 production took place. This effect has been explained by Ozdemir et al. [26] and Basagiannis et al. [19]. They suggest that Mg(II) promotes the adsorption of O_2 or —OH fragments and also their mobility on the catalytic surface, facilitating carbon gasification.

The amount of carbon formed during reaction per gram of catalyst after four hours of reaction is shown in Table 2. However as glycerol total conversion differs for each catalyst, the amount of carbon formed during reaction was normalized by the total conversion of glycerol. These results are also shown in Table 2. The catalyst without Mg(II) presented the highest amount of carbon formed during the steam reforming of glycerol per mol of converted glycerol, whereas the lowest carbon formation per mol of converted glycerol was observed for the catalyst modified with 15 wt% of Mg(II). Concerning the other catalysts with Mg(II) content

Table 2
TPO results. Carbon formation per gram of catalyst and carbon formation per gram of catalyst normalized by glycerol total conversion.

Catalysts	g_C/g_{cat}	x_T (%)	$g_C/(g_{CAT} \times x_T)$
Ni(10)Mg(3)Al	0.07	91.2	0.08
Ni(10)Mg(5)Al	0.07	82.8	0.08
Ni(10)Mg(10)Al	0.05	76.8	0.06
Ni(10)Mg(15)Al	0.03	75.6	0.04
Ni(10)Al	0.07	79.1	0.09

between 3 wt% and 15 wt%, carbon formation per mol of converted glycerol decreased with higher amounts of Mg(II). It is known the importance of Ni particle size on coke formation; however these results showed that carbon formation during glycerol reforming could be explained mainly in terms of the higher basicity of the support, instead that on the differences in particle size. Thus it is evidently that exist a correlation between the basicity of the support and carbon formation, whereas there is not clear correlation between carbon formation and Ni particle size.

Therefore, based on these results a controversy is established. If the aim is to minimize carbon formation, higher contents of Mg(II) should be used, whereas if the goal is to achieve better catalytic activity for the GSR, lower Mg(II)/Al(III) ratios should be employed.

Samples with varying content of Mg(II), either used or fresh, were analyzed by scanning electron microscopy. From the SEM images corresponding to the catalysts with Mg(II), it was possible to determine that there were no significant differences between these fresh catalysts. All samples exhibit a sheet like structure combined with granules (Figs. 11 and 12).

The used samples clearly differ from the fresh ones, since regardless the content of Mg(II) the sheet-like structure disappeared and it

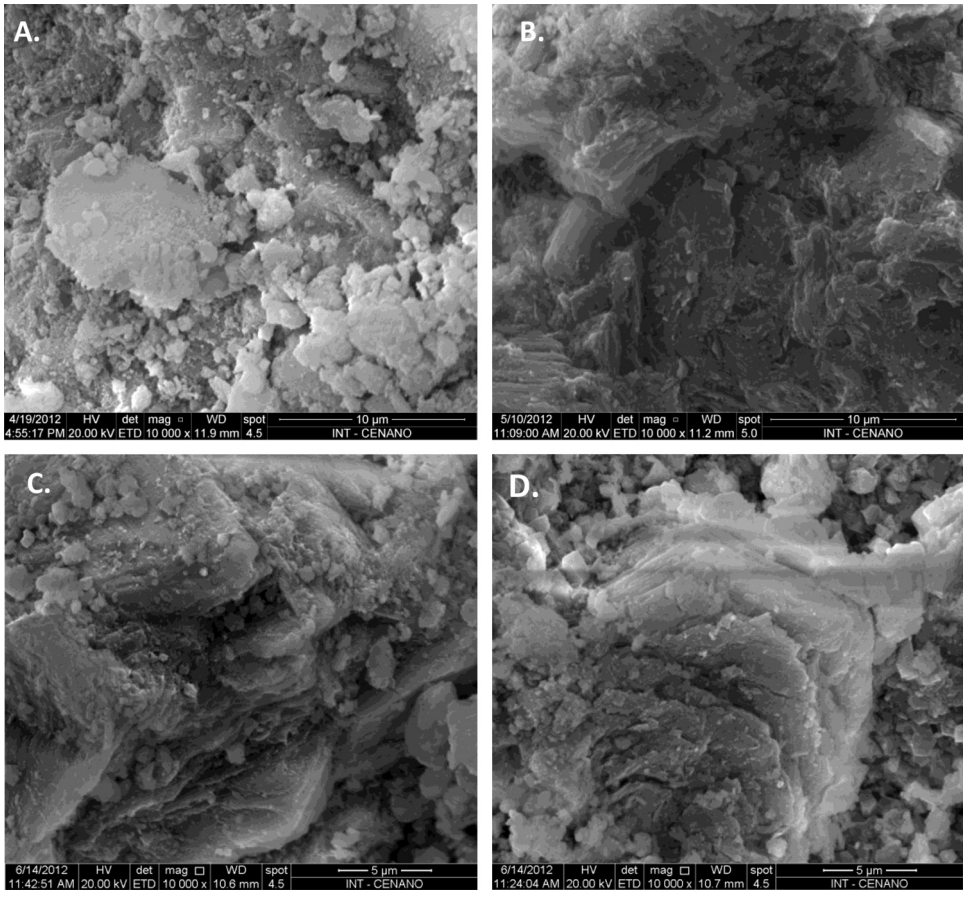

Fig. 11. SEM images of the fresh catalysts. Ni(10)Mg(x)Al, A: x = 3 wt%, B: x = 5 wt.%, C: x = 10 wt.% and D: x = 15 wt.%.

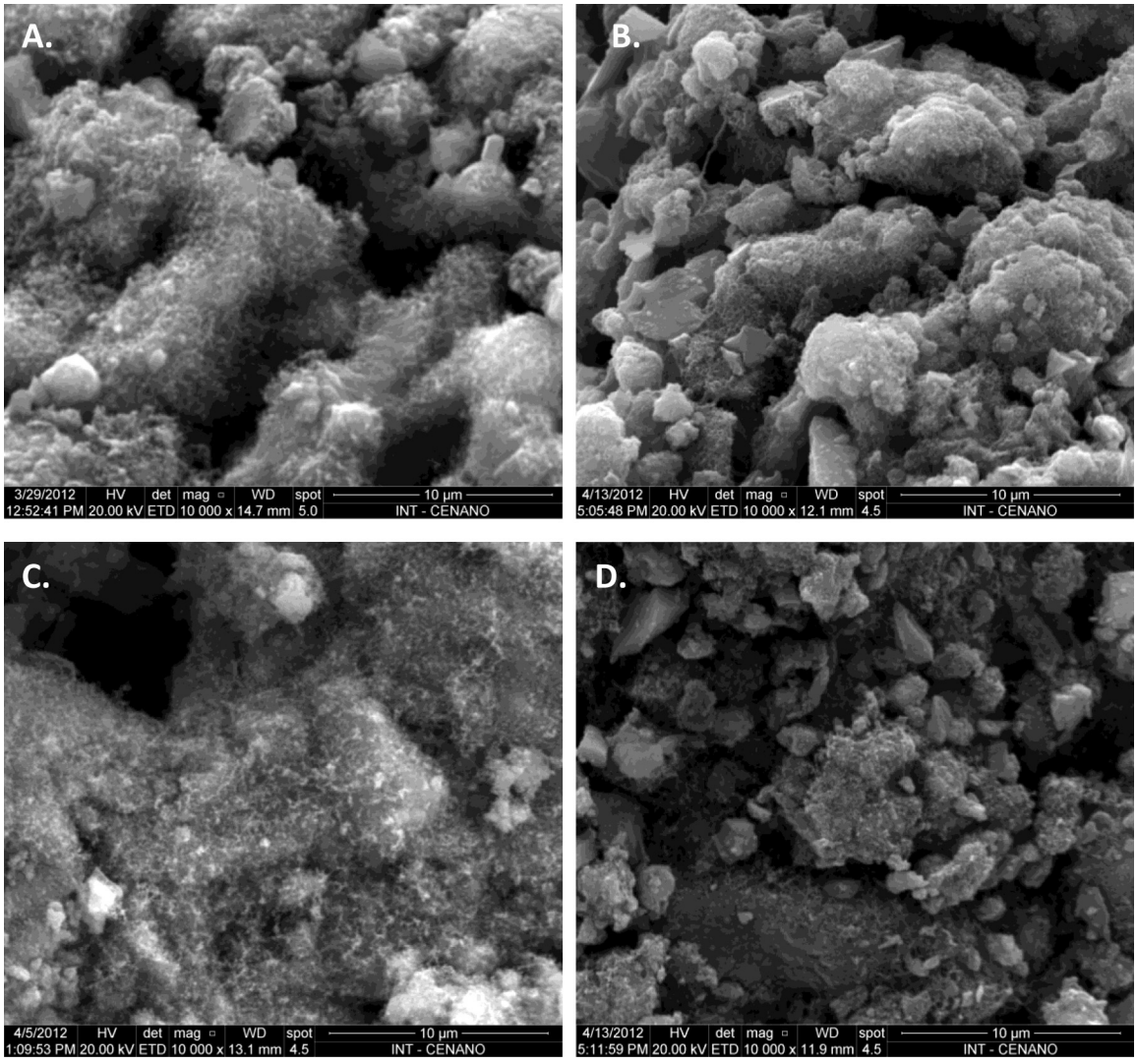

Fig. 12. SEM images of the used catalysts. Ni(10)Mg(x)Al, A: x = 3 wt%, B: x = 5 wt.%, C: x = 10 wt.% and D: x = 15 wt.%.

was only possible to appreciate the granular type structure. Added to this, for the catalysts with a content of Mg(II) between 3 wt% and 10 wt%, filaments of carbon (whisker) were observable. Carbon filaments were not observed for the catalysts 15 wt%. Although, based on the TPO profiles, the formation of these filaments should not be discarded.

4. Conclusions

The effect of Mg(II) as a promoter of Ni based catalysts supported over alumina and of its content, on both, the catalytic activity and carbon deposition in the steam reforming of glycerol is studied. Loading the support (γ-Al_2O_3) with Mg(II) promoted the formation of Mg(II) spinel ($Mg_{1-x}Al_2O_{4-x}$), which is a phase with high inherent stability. Nevertheless, H_2 chemisorption revealed that Ni metallic area and Ni dispersion were enhanced at low contents of Mg(II). Consequently, in order to obtain a catalysts with high metal dispersion that favours glycerol conversion to gaseous products it is advisable to modify the support with low percentages of Mg(II).

For the catalysts modified with Mg (II) there is a linear relation between the conversion to gaseous products and Ni dispersion. This behaviour could suggests that these catalysts have the same type of Ni(0) active sites. While the deviation from this linear relation detected for the catalyst without Mg (II) might imply that this catalyst has a different type of active Ni(0) site and particularly more active and more strongly deactivated by carbon formation than the one in catalysts modified. Thus, it is could be concluded that the catalytic activity is related with the Ni(0) particle obtained from reduction of NiO with weak interaction with support, but this species presents different intrinsic activity depending on if the alumina is modified with Mg(II).

Concerning catalyst deactivation, the lower amount of carbonaceous deposits was formed with the catalyst with the highest Mg (II) loading. Therefore, carbon formation could be related to the basic character of the catalysts; the higher basicity of the support and the promoting effect of Mg might favour carbon gasification during steam reforming of glycerol.

Finally, it should be noted that the optimum catalytic performance was obtained with the 3 wt% Mg(II) modified support with an H_2 yield of 4.8, which corresponds to 77% of the thermodynamic yield under these conditions. Also the conversion to gaseous products for this catalyst was 79.3% and conversion to liquid products corresponded to the minimum recorded (about 11%).

Acknowledgments

To CONICET, ANPCyT and University of Buenos Aires for financial support. To Peruilh Foundation for Maria Laura Dieuzeide scholarship.

We would like to thank Andrea María Duarte de Farias, for the SEM analysis.

References

[1] M.L. Dieuzeide, N.E. Amadeo, Chemical Engineering and Technology 33 (1) (2010) 89–96.
[2] S. Adhikari, S. Fernando, A. Haryanto, Catalysis Today 129 (2007) 355–364.
[3] S. Czernik, R. French, C. Feik, E. Chornet, Industrial and Engineering Chemistry Research 41 (2002) 4209–4215.
[4] T. Hirai, N. Ikenaga, T. Miyake, T. Suzuki, Energy and Fuels 19 (2005) 1761–1762.
[5] R.R. Soares, D.A. Simonetti, J.A. Dumesic, Angewandte Chemie International Edition 45 (2006) 3982–3985.
[6] D.A. Simonetti, E.L. Kunkes, J.A. Dumesic, Journal of Catalysis 247 (2007) 298–306.
[7] E.L. Kunkes, R.R. Soares, D.A. Simonetti, J.A. Dumesic, Applied Catalysis B 90 (2009) 693–698.
[8] S. Adhikari, S.D. Fernando, S.D. Filip To, R.M. Bricka, P.H. Steele, A. Haryanto, Energy and Fuels 22 (2008) 1220–1226.
[9] A. Iriondo, V.L. Barrio, J.F. Cambra, P.L. Arias, M.B. Guemez, R.M. Navarro, M.C. Sanchez-Sanchez, J.L.G. Fierro, Topics in Catalysis 49 (2008) 46–58.
[10] F. Aupretre, C. Descorme, D. Duprez, D. Casanave, D.J. Uzio, Journal of Catalysis 233 (2005) 464–477.
[11] A. Iriondo, M.B. Guemez, V.L. Barrio, J.F. Cambra, P.L. Arias, M.C. Sánchez-Sánchez, R.M. Navarro, J.L.G. Fierro, Scientific Bases for the Preparation of Heterogeneous Catalysts, vol. 175, Elsevier, Amsterdam, 2010, pp. 449–452.
[12] K. Young Koo, H.S. Roh, Y. Taek Seo, D. Joo Seo, W. Lai Yoon, S. Bin Park, Applied Catalysis A 340 (2008) 183–190.
[13] Z. Cheng, Q. Wu, J. Li, Q. Zhu, Catalysis Today 30 (1996) 147–155.
[14] A.L. Alberton, M.M.V.M. Souza, M. Schmal, Catalysis Today 123 (2007) 257–264.
[15] S. Wang, G.Q. Lu, Journal of Chemical Technology and Biotechnology 75 (2000) 589–595.
[16] A. Iriondo, V.L. Barrio, J.F. Cambra, P.L. Arias, M.B. Guemez, M.C. Sanchez-Sanchez, R.M. Navarro, J.L.G. Fierro, International Journal of Hydrogen Energy 35 (2010) 11622–11633.
[17] M.C. Sánchez-Sánchez, R.M. Navarro, J.L.G. Fierro, International Journal of Hydrogen Energy 32 (2007) 1462–1471.
[18] L.P.R. Profeti, E.A. Ticianelli, E.M. Assaf, International Journal of Hydrogen Energy 34 (2009) 5049–5060.
[19] A.C. Basagiannis, X.E. Verykios, Catalysis Today 127 (2007) 256–264.
[20] J.R. Rostrup-Nielsen, J. Sehested, Advances in Catalysis 47 (2002) 65–139.
[21] M.L. Dieuzeide, V. Iannibelli, M. Jobbagy, N. Amadeo, International Journal of Hydrogen Energy 37 (2012) 14926–14930.
[22] F. Patcas, D. Hönicke, Catalysis Communications 6 (2005) 23–27.
[23] F. Pompeo, G.F. Santori, N.N. Nichio, Catalysis Today 172 (2011) 183–188.
[24] B. Kitiyanan, W.E. Alvarez, J.H. Harvell, D.E. Resasco, Chemical Physics Letters 317 (2000) 497–503.
[25] S.M. de Lima, A.M. da Silva, L.O.O. da Costa, U.M. Graham, G. Jacobs, B.H. Davis, L.V. Mattos, F.B. Noronha, Journal of Catalysis 268 (2009) 268–281.
[26] H. Ozdemir, M.A. Faruk Öksüzömer, M. Ali Gürkaynak, International Journal of Hydrogen Energy 35 (2010) 12147–12160.